Iterative Joint-Over-Antenna Detection and WNRA Decoding in Single-Carrier Multiuser MIMO Systems

Kai Yen, Nenad Veselinovic, *Member, IEEE*, Kimmo Kansanen, and Tadashi Matsumoto, *Senior Member, IEEE*

***Abstract*—In this paper, we propose a combined iterative detection and decoding technique that is capable of achieving the maximum diversity of order $N_T \times L \times N_R$ over single-carrier multiple-input–multiple-output (MIMO) frequency-selective Rayleigh fading channels, where N_T and N_R denote the number of transmit and receive antennas, respectively, and L is the number of multipath components. The so-called space-time weighted-nonbinary-repeat-accumulate (ST-WNRA) codes are considered in our paper due to their ability to provide a full transmit antenna diversity and their relatively simple encoding and decoding algorithms. Multipath diversity is obtained using a joint-over-antenna turbo-equalization technique based on the minimum-mean-square-error filtering with soft interference cancellation. Computer simulations demonstrate that our proposed turbo-equalized system with ST-WNRA codes is capable of achieving the maximum diversity order with a relatively short codeword length and that the multiuser performance approaches the single-user bound so far as the number of users is smaller than or equal to the number of receive antennas in multiuser MIMO setups. We will also show that by modifying our proposed scheme to an equivalent multilevel coded system, higher bandwidth efficiency can be achieved at the expense of a performance loss while the system still retains the maximum diversity benefit.**

***Index Terms*—Iterative decoding, multilevel coding, multiple-input–multiple-output (MIMO) systems, repeat-accumulate codes, turbo equalization.**

I. Introduction

THE NOTION of diversity has been widely accepted as one of the most important component for reliable wireless communications. Information theoretic aspects of transmit diversity studied by Telatar [1] and Foschini and Gans [2] have demonstrated that the capacity of multiple-input–multiple-output (MIMO) systems significantly exceeds that of single-antenna systems in scattering rich fading channels. These promising results prompted the development of several so-called space-time-coding (STC) schemes, notably space-time trellis codes (STTC) [3] and space-time block codes (STBC) [4]. Most of the STC schemes proposed so far were constructed based on the design criteria derived primarily for narrowband flat fading channels, and they have been shown to achieve at least the full multiantenna diversity order of $N_T \times N_R$ over a flat fading channel, where N_T and N_R denote the number of transmit and receive antennas, respectively.

However, in order to support very high data rates that are expected in future wireless communication systems, MIMO systems will have to operate in much wider bandwidths. This creates the problem of intersymbol interference (ISI) due to the channel's frequency selectivity. It was shown in [5] that conventional STC schemes are still capable of achieving the full multiantenna diversity gain in frequency-selective channels. However, the coding gain decreases significantly due to ISI. Hence, it is natural to assume that the presence of multiple-access interference (MAI) when implemented over a multi-user environment will deteriorate the performance of the STC schemes even further. Moreover, the multipath diversity gain that can be gleaned from frequency-selective channels is not fully exploited by conventional STC schemes.

As noted in [6], designing optimal STC schemes that are capable of exploiting the multipath diversity in frequency-selective channels is a complicated problem. Hence, a more realistic proposition will be to use existing STC designs and, instead, develop more sophisticated but still tractable signal processing algorithms to achieve the maximum diversity order of $N_T \times L \times N_R$, where L is the number of finite-impulse-response channel taps [7]. For instance, based on the pairwise-error-probability analysis, it was shown in [8]–[10] that with STTCs, it is possible to achieve the maximum diversity order in an orthogonal-frequency-division-multiplexing (OFDM)-based MIMO system, given that the rank of the codeword-difference matrix is LN_T. This requirement would entail large-size codewords. Furthermore, OFDM-based techniques have high peak-to-average ratio, and their performances are sensitive to carrier-synchronization error [11]. On the other hand, novel transmission schemes based on STBC that are capable of achieving the maximum diversity order were proposed in [6] and [12] and, more recently, in [13]. Unfortunately, these schemes suffer a loss in bandwidth efficiency due to the utilization of STBCs. Furthermore, it is not known how these schemes will perform under a multiple-access environment.

Hence, to address the shortcomings of those systems, in this paper, we proposed a bandwidth-efficient system that is also capable of achieving the maximum diversity order

Manuscript received May 24, 2005; revised April 13, 2006 and April 14, 2006. The review of this paper was coordinated by Prof. Z. Wang.

K. Yen is with the Institute for Infocomm Research, Singapore 119613 (e-mail: yenkai@i2r.a-star.edu.sg).

N. Veselinovic is with the Elektrobit Ltd., 02700 Kauniainen, Finland (e-mail: nenad.veselinovic@elektrobit.com).

K. Kansanen and T. Matsumoto are with the University of Oulu, 90014 Oulu, Finland (e-mail: kmo@ee.oulu.fi; tadashi.matsumoto@ee.oulu.fi).

Color versions of one or more of the figures in this paper are available online at http://ieeexplore.ieee.org.

Digital Object Identifier 10.1109/TVT.2007.891441

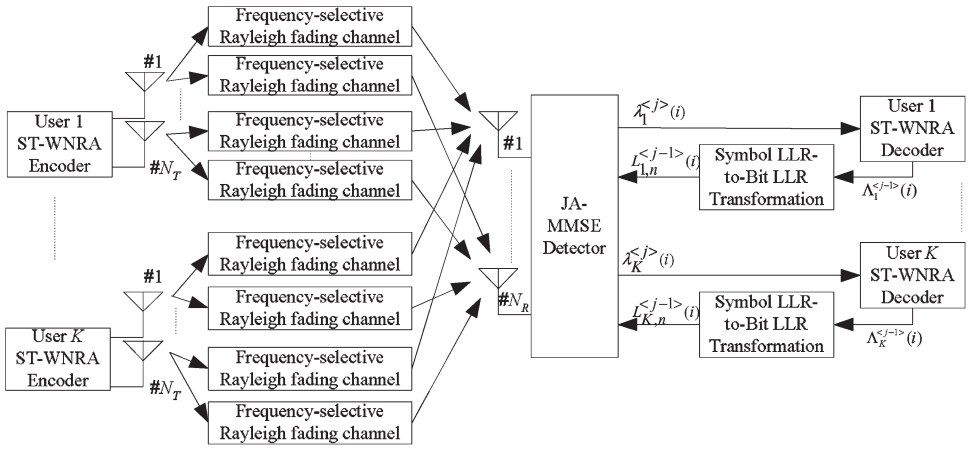

Fig. 1. ST-WNRA-coded mulituser MIMO system model.

over a frequency-selective Rayleigh fading channel, regardless of the codeword dimensionality. More explicitly, multipath diversity is not obtained directly from the codeword itself. Hence, codewords having a rank of N_T is always sufficed. Specifically, transmit diversity is obtained by utilizing the so-called space-time weighted-nonbinary repeat-accumulate (ST-WNRA) codes, invented by Oh and Yang in [14], where it was shown that these codes have a rank equivalent to $\min(r, N_T)$ as well as a rate given by N_T/r for any codeword length, where r is the number of symbol repetitions. Furthermore, instead of invoking the maximum *a posteriori* decoder, ST-WNRA codes can be efficiently decoded using the sum–product algorithm [14].

In our proposed system, the multipath diversity that is available from the received signal will be fully exploited by transforming the frequency-selective faded desired signal to a vector of flat faded signals, which is then utilized by the ST-WNRA decoder to achieve the maximum diversity order. The requirement on our proposed system is that these flat faded signals must contain as little interference (ISI and MAI) as possible so that the ST-WNRA decoder can converge toward the maximum diversity order. This requirement can be fulfilled by using a joint-over-antenna turbo-equalization technique based on the minimum mean-square-error filtering (JA-MMSE) with soft interference cancellation [15] performed before the ST-WNRA decoder, whereby the symbols transmitted from all the antennas of each user during the same signaling interval will be detected jointly by the JA-MMSE detector. Extrinsic information is exchanged between the ST-WNRA decoder and the JA-MMSE detector in an iterative manner in order to improve the mutual information and, hence, leads to convergence. While equalization techniques for realizing STC in frequency-selective channels have already been proposed [16]–[18] (see [19] for an overview treatment), the multipath diversity gain is not exploited in these equalization techniques. Furthermore, multiple access was not considered in these treatises.

We will show that by using the JA-MMSE detection technique in conjunction with the ST-WNRA codes, the overall proposed system is capable of achieving the maximum diversity order at a bandwidth efficiency higher than that offered by STBCs and also at relatively short codeword length. Unlike the coded-OFDM systems where the purpose of the interleaver is to provide randomness of the channel, the interleaver in our proposed system is to improve the decoder feedback mutual information in order for the JA-MMSE detector to effectively convert the L-path channels to the equivalent LN_R flat channels to achieve maximum diversity order. Hence, asymptotically, our proposed system can achieve the maximum diversity order with any frame length. Furthermore, the multiuser performance approaches the single-user bound as long as N_R equals to the number of users present. We will also briefly highlight and illustrate through simulations that our proposed space-time multiple-access transceiver can be modified to an equivalent multilevel coded system such that the bandwidth efficiency of the system can be further enhanced at the expense of a performance loss. This bandwidth-efficiency–bit-error rate (BER) tradeoff is attained without suffering any loss in the achievable maximum diversity order.

This paper is organized as follows. Section II describes the frequency-selective multiuser MIMO channel model assumed in this paper. In Section III, the JA-MMSE detector will be presented. The emphasis here will be on ISI and MAI suppression and also on how maximum diversity order can be guaranteed. Simulation results illustrating the BER performance of our proposed system are given in Section IV. Following this, a brief discourse on the modification of our proposed transceiver to an equivalent multilevel coded system will be given in Section V. Some simulation results will also be shown. Finally, a summary and the conclusions are given in Section VI.

II. System Model

We consider the uplink of a single-cell synchronous K-user single-carrier MIMO channel, where N_T transmit antennas and N_R receive antennas are located at each user and at the base station, respectively, as shown in Fig. 1.

Let $\mathbf{u}_k = [u_k(1), \ldots, u_k(N)]$ be a frame of N uncoded information symbols corresponding to the kth user to be encoded, where $u_k(i) \in \mathrm{GF}(2^q)$, with q being a positive integer. Note that each symbol in turn corresponds to q number of information bits. Basically, the ST-WNRA encoder employed here is

the same as that used in [14], which is highlighted in Appendix I in this paper. In general, as given by (31) in Appendix I, we can expressed the kth user's ST-WNRA codeword as an $N_T \times rN$ matrix $\mathbf{C}_k$ as follows:

$$\mathbf{C}_k = \begin{bmatrix} c_{k,1}(1) & c_{k,1}(2) & \cdots & c_{k,1}(rN) \\ \vdots & \vdots & \ddots & \vdots \\ c_{k,N_T}(1) & c_{k,N_T}(2) & \cdots & c_{k,N_T}(rN) \end{bmatrix} \quad (1)$$

where $c_{i,j}(\gamma) \in \{-1, +1\}$ for $i = 1, \ldots, K$, $j = 1, \ldots, N_T$, and $\gamma = 1, \ldots, rN$, and r denotes the number of symbol repetitions in the encoder. Each row in $\mathbf{C}_k$ is assigned to a distinct transmit antenna. Independent ST-WNRA codewords will be transmitted by all K users from their corresponding N_T antennas at the same time and frequency without spreading. It was shown in [14] that the ST-WNRA codeword $\mathbf{C}_k$ has a rank given by $\min(r, N_T)$, and this determines the achievable transmit diversity order. Also, the codeword has a rate of N_T/r. Hence, if $N_T = r$, a full-rate ST-WNRA code having full-transmit-antenna-diversity advantage is obtained.

A. Spatially Independent Channel

Due to multipath propagation and assuming that the antennas are sufficiently separated, the channel between each transmit–receive antenna pair can be considered as suffering from independent frequency-selective Rayleigh fading. Without loss of generality, the number of multipath components L is assumed to be common to all transmit–receive antenna pairs and that the channel is quasi-static. The lth complex path gain between the kth user's nth transmit antenna and the mth received antenna is denoted by $h_{k,n}^{(m)}(l)$, and these path gains are modeled as samples of independent zero-mean complex Gaussian random variables. The received signal at the mth receive antenna during the ith signaling interval is a noisy superposition of $K \times L \times N_T$ independent Rayleigh faded signals, which is given by

$$r^{(m)}(i) = \sum_{k=1}^{K} \sum_{n=1}^{N_T} \sum_{l=0}^{L-1} h_{k,n}^{(m)}(l) c_{k,n}(i-l) + v^{(m)}(i) \quad (2)$$

where $v^{(m)}(i)$ is the additive white Gaussian noise. The equivalent vector representation of the received signals at the ith signaling interval can be written as

$$\mathbf{r}(i) \equiv \left[r^{(1)}(i), \ldots, r^{(N_R)}(i)\right]^{\mathrm{T}} = \sum_{l=0}^{L-1} \mathbf{H}(l)\mathbf{c}(i-l) + \mathbf{v}(i) \quad (3)$$

where

$$\begin{aligned} \mathbf{H}(l) &= [\mathbf{H}_1(l), \ldots, \mathbf{H}_k(l), \ldots, \mathbf{H}_K(l)] \\ \mathbf{H_k}(l) &= \left[\mathbf{h}_k^{(1)}(l), \ldots, \mathbf{h}_k^{(N_R)}(l)\right]^{\mathrm{T}} \\ \mathbf{h}_k^{(m)}(l) &= \left[h_{k,1}^{(m)}(l), \ldots, h_{k,N_T}^{(m)}(l)\right]^{\mathrm{T}} \end{aligned} \quad (4)$$

and

$$\mathbf{c}(i) = [\mathbf{c}_1(i), \ldots, \mathbf{c}_K(i)]^{\mathrm{T}} \; ; \mathbf{c}_k(i) = [c_{k,1}(i), \ldots, c_{k,N_T}(i)]. \quad (5)$$

From (3), temporal sampling is then performed to capture the multipath signals corresponding to the ith signaling interval for diversity combining, which yields the following space-time received-signal vector:

$$\mathbf{y}(i) \equiv \left[\mathbf{r}^{\mathrm{T}}(i+L-1), \ldots, \mathbf{r}^{\mathrm{T}}(i)\right]^{\mathrm{T}} = \mathbf{H}\mathbf{b}(i) + \mathbf{n}(i) \quad (6)$$

where

$$\mathbf{H} = \begin{bmatrix} \mathbf{H}(0) & \ldots & \mathbf{H}(L-1) & \cdots & \mathbf{0} \\ \vdots & \ddots & \vdots & \ddots & \vdots \\ \mathbf{0} & \cdots & \mathbf{H}(0) & \cdots & \mathbf{H}(L-1) \end{bmatrix} \quad (7)$$

$$\mathbf{b}(i) = \left[\mathbf{c}^{\mathrm{T}}(i+L-1), \ldots, \mathbf{c}^{\mathrm{T}}(i), \ldots, \mathbf{c}^{\mathrm{T}}(i-L+1)\right]^{\mathrm{T}} \quad (8)$$

and

$$\mathbf{n}(i) = \left[\mathbf{v}^{\mathrm{T}}(i+L-1), \ldots, \mathbf{v}^{\mathrm{T}}(i)\right]^{\mathrm{T}}. \quad (9)$$

Note that in a single-user flat fading channel, where $L = 1$ and $K = 1$

$$\mathbf{y}(i) = \mathbf{H}_1(0)\mathbf{c}_1^{\mathrm{T}}(i) + \mathbf{v}(i). \quad (10)$$

Under this channel condition, full multiantenna diversity of order $N_T \times N_R$ can be achieved, as we shall see later in Section IV.

B. Spatially Correlated Channel

The assumption of a spatially independent channel holds as long as there is sufficient separation among the antennas. However, in the event of insufficient antenna spacing, this assumption is no longer true and the channel is spatially correlated. It has been shown in [20] and [21] that the presence of spatial fading correlation can degrade the performance of STC. Assuming a flat fading channel for simplicity, the model for an $N_R \times N_T$ correlated channel can be written as [20]

$$\mathbf{H} = \mathbf{R}_R^{1/2} \mathbf{H}_w \mathbf{R}_T^{1/2} \quad (11)$$

where $\mathbf{R}_R$ and $\mathbf{R}_T$ are the receive and transmit correlation matrices, and $\mathbf{H}_w$ is an $N_R \times N_T$ independent and identically distributed zero-mean complex Gaussian matrix. In this paper, we only focus on receive antenna correlation such that $\mathbf{R}_T = \mathbf{I}_{N_T \times N_T}$, and

$$\mathbf{R}_R = \begin{bmatrix} 1 & \rho_{1,2} & \cdots & \rho_{1,N_R} \\ \rho_{2,1} & 1 & \cdots & \rho_{2,N_R} \\ \vdots & \vdots & \ddots & \vdots \\ \rho_{N_R,1} & \rho_{N_R,2} & \cdots & 1 \end{bmatrix} \quad (12)$$

where $\rho_{n,m}$ denotes the correlation coefficient between the nth and mth receive antenna. It can be seen that (11)

gives a generalized expression of the MIMO channel since, if $\rho_{n,m} = 0$ for $n \neq m$, the channel becomes uncorrelated. Kermoal *et al.* [22] gave a good account on the generation of the correlated channel gains, which we have adopted in our simulations.

III. JA-MMSE Turbo Equalization With ST-WNRA Codes

The iterative JA-MMSE equalization and ST-WNRA decoding structure is shown in Fig. 1. Basically, it consists of a JA-MMSE detector, followed by K parallel ST-WNRA decoders. In general, the inputs to the JA-MMSE detector comprise the temporal-sampled received signals from the N_R receive antennas, as given by (6), and the *a priori* log-likelihood ratio (LLR) information of the coded binary phase-shift keying (BPSK) symbols of all users, which is denoted by $L_{k,n}^{\langle j-1\rangle}(i)$, $i = 1, \ldots, rN$ in Fig. 1. The *a priori* LLR information was fed back from the K single-user ST-WNRA decoders in the previous iteration via the symbol LLR-to-bit LLR transformer. The superscript $\langle j\rangle$ denotes the jth iteration. Based on these inputs, the JA-MMSE detector computes the extrinsic LLR information of the coded GF(2^q) symbols $\lambda_k^{\langle j\rangle}(i)$, $i = 1, \ldots, rN$, which is then fed to the kth user's ST-WNRA decoder, as illustrated in Fig. 1. The ST-WNRA decoder of the kth user proceeds to compute a new set of extrinsic LLR information corresponding to its transmitted ST-WNRA codeword, which is then transferred to the JA-MMSE detector as *a priori* information for the utilization in the next iteration.

A. JA-MMSE Detector

The general structure of the JA-MMSE detector follows our work in [15], which in some ways, is similar to that found in [23] and [24]. Let us assume that the kth user is the user of interest and that the JA-MMSE detector is currently detecting the transmitted BPSK symbols during the ith transmission period, i.e., $[c_{k,1}(i), \ldots, c_{k,N_T}(i)]^{\mathrm{T}}$. At the jth iteration, the extrinsic LLR information of the coded BPSK symbols provided by the K ST-WNRA decoders from the previous iteration via the symbol LLR-to-bit LLR transformer can be expressed as

$$L_{k,n}^{\langle j-1\rangle}(i) = \log \frac{P\left[c_{k,n}(i) = +1\right]}{P\left[c_{k,n}(i) = -1\right]} \quad k = 1, \ldots, K; \quad n = 1, \ldots, N_T \quad i = 1, \ldots, rN. \tag{13}$$

For the first iteration, assuming equal probability, $L_{k,n}^{\langle 0\rangle}(i) = 0\ \forall k, n, i$, since no prior information about the coded BPSK symbols is available. As we have mentioned before, the objective of the JA-MMSE detector is to suppress the MAI and ISI, as well as to transform the frequency-selective fading channel of the desired user to the equivalent flat fading channel in order to fully exploit the multipath diversity that is available with the received signal. A bulk of the interferences can be suppressed from the desired signal using soft cancellation. Based on the extrinsic LLR information given in (13), the JA-MMSE first forms soft estimates of the transmitted BPSK symbols of all the users as follows:

$$\tilde{c}_{t,n}^{\langle j\rangle}(i+l) = \begin{cases} \tanh\left\{\frac{L_{t,n}^{\langle j-1\rangle}(i+l)}{2}\right\}, & \text{for } t \neq k \text{ or } l \neq 0 \\ 0, & \text{for } t = k \text{ and } l = 0. \end{cases} \tag{14}$$

Using these soft estimates, the interfering users' transmitted signals, as well as the desired user's own ISI, are then estimated and suppressed from the received signal accordingly, as given by

$$\tilde{\mathbf{y}}_k^{\langle j\rangle}(i) = \mathbf{y}(i) - \mathbf{H}\tilde{\mathbf{b}}^{\langle j\rangle}(i) \tag{15}$$

where

$$\tilde{\mathbf{b}}^{\langle j\rangle}(i) = \left[\tilde{\mathbf{c}}^{\langle j\rangle}(i+L-1), \ldots, \tilde{\mathbf{c}}^{\langle j\rangle}(i), \ldots, \tilde{\mathbf{c}}^{\langle j\rangle}(i-L+1)\right]^{\mathrm{T}} \tag{16}$$

with

$$\tilde{\mathbf{c}}^{\langle j\rangle}(i+l) = \left[\tilde{\mathbf{c}}_1^{\langle j\rangle}(i+l), \ldots, \tilde{\mathbf{c}}_k^{\langle j\rangle}(i+l), \ldots, \tilde{\mathbf{c}}_K^{\langle j\rangle}(i+l)\right]$$
$$\tilde{\mathbf{c}}_k^{\langle j\rangle}(i+l) = \left[\tilde{c}_{k,1}^{\langle j\rangle}(i+l), \ldots, \tilde{c}_{k,N_T}^{\langle j\rangle}(i+l)\right]. \tag{17}$$

It can be observed from (14) that $\tilde{\mathbf{c}}_k^{\langle j\rangle}(i)$ is a zero vector so that the desired signal will not be cancelled from $\mathbf{y}(i)$. Due to the nature of the soft estimates, as opposed to hard estimates as well as some erroneous cancellations, there will still be some interferences residing in $\tilde{\mathbf{y}}_k^{\langle j\rangle}(i)$. Hence, an MMSE filter is invoked in order to suppress these residual interferences. More explicitly, the filter weighting matrix $\mathbf{w}_k^{\langle j\rangle}(i)$ is derived according to the following minimization criterion:

$$\mathbf{w}_k^{\langle j\rangle}(i) = \arg \min_{\mathbf{w}_k^{\langle j\rangle}(i)} E\left\{\left\|\mathbf{w}_k^{\langle j\rangle^H}(i)\tilde{\mathbf{y}}_k^{\langle j\rangle}(i) - \mathbf{A}_k\mathbf{c}_k^T(i)\right\|^2\right\} \tag{18}$$

where the matrix $\mathbf{A}_k$ is defined as

$$\mathbf{A}_k = \left[\mathbf{H}_k^T(L-1), \ldots, \mathbf{H}_k^T(0)\right]^{\mathrm{T}} \tag{19}$$

with $\mathbf{H}_k(l)$ and $\mathbf{c}_k(i)$ given in (4) and (5), respectively. Notice that our criterion of (18) is different from that used in [23] and [24]. Unlike the criterion used in [23] and [24], where the MMSE turbo detector was used to detect the symbols antenna by antenna, the objective of our JA-MMSE detector in this case is to simply transform $\tilde{\mathbf{y}}_k^{\langle j\rangle}(i)$ into a vector consisting of LN_R number of flat faded desired signals that are free from any interference components. In other words, the term $\mathbf{A}_k\mathbf{c}_k^T(i)$ can be interpreted as transmitting the vector of coded BPSK symbols $\mathbf{c}_k(i)$ over a flat fading channel and received by LN_R number of antennas, where the flat fading coefficients are defined by $\mathbf{A}_k$. By doing this, it has been shown analytically in [15] that the asymptotic performance of the MMSE turbo equalizer approaches the maximum diversity order of LN_R. Hence, by incorporating the ST-WNRA in our design, a maximum diversity order of $N_T \times L \times N_R$ can be asymptotically achieved. It can

be shown that the weighting matrix $\mathbf{w}_k^{\langle j\rangle}(i)$ that satisfies (18) is given by [15]

$$\mathbf{w}_k^{\langle j\rangle}(i) = \left[\mathbf{H}\mathbf{V}_k^{\langle j\rangle}(i)\mathbf{H}^H + \sigma^2\mathbf{I}\right]^{-1}\mathbf{A}_k\mathbf{A}_k^H \tag{20}$$

where

$$\begin{aligned}\mathbf{V}_k^{\langle j\rangle}(i) = \text{diag}\Bigg\{ & 1 - \left[\tilde{c}_{1,1}^{\langle j\rangle}(i+L-1)\right]^2, \ldots, 1 \\ & - \left[\tilde{c}_{1,N_T}^{\langle j\rangle}(i+L-1)\right]^2, \ldots, 1 \\ & - \left[\tilde{c}_{K,N_T}^{\langle j\rangle}(i-L+1)\right]^2 \Bigg\}.\end{aligned} \tag{21}$$

Hence, the instantaneous MMSE estimate of the kth user's signal during the ith transmission period, which is denoted as $\mathbf{z}_k^{\langle j\rangle}(i)$, is given by

$$\mathbf{z}_k^{\langle j\rangle}(i) = \mathbf{w}_k^{\langle j\rangle^H}(i)\tilde{\mathbf{y}}_k^{\langle j\rangle}(i). \tag{22}$$

For the BPSK-coded vector $\mathbf{c}_k(i)$, the vector $\mathbf{z}_k^{\langle j\rangle}(i)$ can be modeled as a Gaussian process [15] having a mean $\mathbf{\Omega}_k^{\langle j\rangle}(i)\mathbf{c}_k^T(i)$, where

$$\mathbf{\Omega}_k^{\langle j\rangle}(i) = \mathbf{w}_k^{\langle j\rangle^H}(i)\mathbf{A}_k \tag{23}$$

and a covariance matrix

$$\mathbf{\Theta}_k^{\langle j\rangle}(i) = \mathbf{\Omega}_k^{\langle j\rangle}(i)\left\{\mathbf{A}_k^H - \mathbf{\Omega}_k^{\langle j\rangle^H}(i)\right\}. \tag{24}$$

Based on the Gaussian assumption of $\mathbf{z}_k^{\langle j\rangle}(i)$, we can calculate the extrinsic LLR vector of the transmitted coded GF(2^q) symbols $\lambda_k^{\langle j\rangle}(i) \equiv [\lambda_k^{\langle j\rangle}(i,0), \ldots, \lambda_k^{\langle j\rangle}(i,2^q-1)]$, where the index (i,n) denotes the nth element in the LLR vector for the ith coded GF(2^q) symbol, and $\lambda_k^{\langle j\rangle}(i,n)$ is given by

$$\lambda_k^{\langle j\rangle}(i,n) = \log\frac{P\left(c_k(i) = C_n|\mathbf{z}_k^{\langle j\rangle}(i)\right)}{P\left(c_k(i) = C_0|\mathbf{z}_k^{\langle j\rangle}(i)\right)}, \text{ for } n = 0, \ldots, 2^q-1 \tag{25}$$

and

$$\begin{aligned}P\left(c_k(i) = C_n|\mathbf{z}_k^{\langle j\rangle}(i)\right) = \chi\exp\Bigg\{ & -\left[\mathbf{z}_k^{\langle j\rangle}(i) - \mathbf{\Omega}_k^{\langle j\rangle}(i)\bar{\mathbf{c}}_n\right]^{\text{H}} \\ & \times \mathbf{\Theta}_k^{-1}(i)\left[\mathbf{z}_k^{\langle j\rangle}(i) - \mathbf{\Omega}_k^{\langle j\rangle}(i)\bar{\mathbf{c}}_n\right]\Bigg\}\end{aligned} \tag{26}$$

where $\bar{\mathbf{c}}_n = [c_n(1), \ldots, c_n(N_T)]^{\text{T}}$, $c_n(t) \in \{+1, -1\}$; $t = 1, \ldots, N_T$ is a BPSK representation of C_n, and χ is the normalization factor, which cancels itself out in (25). Obviously, from (25), $\lambda_k^{\langle j\rangle}(i,0) = 0$. The coded GF($2^q$) symbol LLR vector of each user is calculated for the entire frame before passing to the corresponding user's ST-WNRA decoder, as shown in Fig. 1.

B. ST-WNRA Decoder

Similar to the low-density parity-check (LDPC) codes [25], ST-WNRA codes can be efficiently decoded using the so-called sum–product algorithm. Description of the sum–product algorithm for the ST-WNRA decoder is given in [14] and can also be found in Appendix II for completeness sake.

The extrinsic information $\Lambda_k^{\langle j\rangle}(i)$ provided by the ST-WNRA decoder, as given in (38), represents the LLR of the coded GF(2^q) symbols. Hence, a symbol LLR-to-binary LLR transformation needs to be carried out, in order to produce the LLR of each coded BPSK symbol $L_{k,n}^{\langle j\rangle}(i), n = 1, \ldots, N_T$ before the information can be used by the JA-MMSE detector, as defined by (14). This transformation is given by [26]

$$L_{k,n}^{\langle j\rangle}(i) = \log\frac{\sum_{d|c_{k,n}(i)=+1} P\left\{d = [c_{k,1}(i), \ldots, c_{k,N_T}(i)]\right\}}{\sum_{d|c_{k,n}(i)=-1} P\left\{d = [c_{k,1}(i), \ldots, c_{k,N_T}(i)]\right\}} \tag{27}$$

for $n = 1, \ldots, N_T$, and $P(d) = \exp[\Lambda_k^{\langle j\rangle}(i,d)]$, with $d \in$ GF(2^q).

C. Complexity

A bulk of the complexity in the JA-MMSE detector comes from the matrix inversion, in order to obtain the filter taps $\mathbf{w}_k^{\langle j\rangle}(i)$, as shown in (20). The complexity required for this operation is in the order of $O\{L^3N_R^3\}$ per coded GF(2^q) symbol per user per iteration. As highlighted in our previous section, the flow of information from the JA-MMSE detector to the ST-WNRA decoder and then back to the JA-MMSE detector constitutes one iteration. On the other hand, it is also possible to iterate the information within the ST-WNRA decoder for several times, in order to improve its reliability before releasing the information to the JA-MMSE detector. This option may reduce the number of times required in performing the matrix inversion at the JA-MMSE detector and, hence, reduced the system complexity. Such approach has been proposed before, for example in [27], for LDPC codes. However, this alternative method is not studied in this paper, but it offers an interesting subject for future research.

Further reduction in complexity can also be achieved by invoking the frequency-domain-equalization techniques [28]. A frequency-domain JA detection with ST-WNRA codes proposed recently in [29] showed that the maximum diversity order given by $N_T \times L \times N_R$ was achieved, an observation which is similar to that of using time-domain equalization methods adopted in this paper, as we shall see in the next section.

In the context of the ST-WNRA decoder, it was shown in [30] that the use of the sum–product algorithm for the accumulator requires about 1/6 less operations per information bit as compared to that of using the Bahl–Cocke–Jelinek–Raviv algorithm with binary-code symbols.

IV. Simulation Results

In this section, we investigate the performance of our proposed system using both GF(4) and GF(8) ST-WNRA codes

having $N_T = 2$ and $N_T = 3$ transmit antennas, respectively. In our simulations, the uncoded frame length N is kept at 180 for GF(4) codes and 120 for GF(8) codes, such that the number of information bits in a frame is kept the same for both the codes. The number of repetitions r for both the codes is maintained at three. Hence, for GF(4) ST-WNRA codes, the achievable rate is 2/3, while full rate is achieved for GF(8) ST-WNRA codes. We also define E_b as the average information-bit energy of each user's signal received by one antenna element. In our simulations, an *ad hoc* scaling factor Q, as highlighted in Appendix II, is sometimes used in order to enhance the iterative processing performance. Unless otherwise specified, the Q factor is always set to one. The BER is used as the measure of performance. One point we want to stress here is that we have assumed a single-carrier quasi-static channel in this paper. It should be noted that the time diversity inherent in the ST-WNRA codes, which can further improve the performance of the codes in nonquasi-static channels, as shown in [14], is not exploited here.

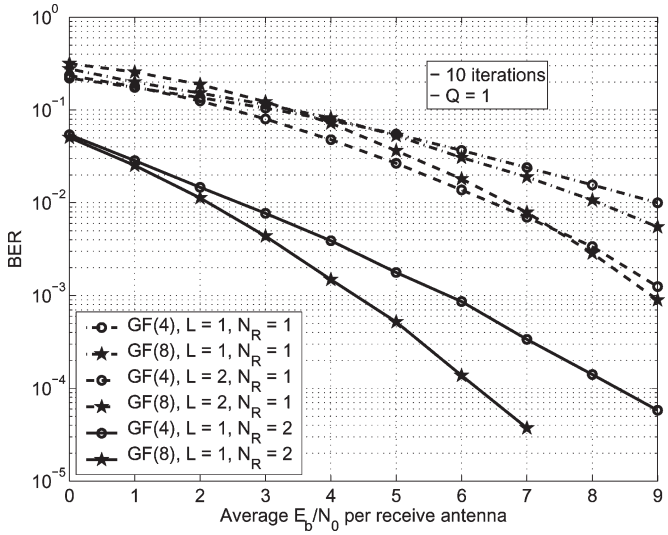

Fig. 2. Performance comparison of GF(4) and GF(8) ST-WNRA codes with (a) $L = 1$ and $N_R = 1$, (b) $L = 2$ and $N_R = 1$, (c) $L = 1$ and $N_R = 2$.

A. Single-User Performance

The results in [14] are only shown with one receive antenna over a flat fading channel. Here, we extended their investigation and illustrate the performance of the ST-WNRA codes with multiple receive antennas in a frequency-selective channel. The objective of these simulations is to see if our proposed system is capable of taking full advantage of the diversity that are available under these conditions, which should be in the order of $N_T \times L \times N_R$, as highlighted previously. These single-user performance results will also be used as bounds for our subsequent investigations in a multiuser environment. In the case of a flat fading channel, there is no ISI. Hence, the JA-MMSE detector is not required and the LLR vector for the ith coded symbol, given in (25), can be directly derived using (26) by replacing $\mathbf{z}_k^{\langle j \rangle}(i)$ and $\mathbf{\Omega}_k^{\langle j \rangle}(i)$ with $\mathbf{y}(i)$ and $\mathbf{H}_1(0)$ of (10), respectively. The covariance matrix is not required here, since it is the same over the entire frame.

Three scenarios are first considered: 1) $L = 1$ and $N_R = 1$; 2) $L = 2$ and $N_R = 1$; and 3) $L = 1$ and $N_R = 2$. The results for 1) were shown in [14] and are reproduced here for comparison sake. The transmit diversity order for GF(4) and GF(8) ST-WNRA codes is two and three, respectively. Hence, for 2) and 3), the maximum achievable diversity order is expected to be four and six for GF(4) and GF(8) codes, respectively, due to the additional diversity obtained from the multipath and the receive antennas [7]. The results are shown in Fig. 2. One obvious observation is that the performance is improved with multipaths as compared to a flat fading channel for a single receive antenna. Hence, with the employment of the JA-MMSE detector, the presence of fading frequency selectivity is actually beneficial for the system-performance enhancement. More importantly, we note that the achievable diversity order is what we have expected. This can be easily seen from Fig. 2 by comparing the slope of the curves for $L = 2$ and $N_R = 1$ and $L = 1$ and $N_R = 2$ for both GF(4) and GF(8) codes, which are corresponding to a diversity order of four and six, respectively. We also noticed that at low E_b/N_0 values when $N_R = 1$, the performance of the GF(4) codes is better than that of the GF(8) codes, but eventually, the GF(8) codes outperform the GF(4) codes at higher E_b/N_0 values.

Recall that the complexity of our proposed iterative system, in particular, the JA-MMSE detector, increases with increased number of multipath components and receive antennas. One way of reducing the complexity of the system is by reducing the number of iterations before making the ultimate decision on the information data, while sacrificing some performance loss. Hence, it is interesting to study the convergence behavior of our system. This is illustrated in Fig. 3(a) and (b) for the case of $L = 2$ and $N_R = 2$ for GF(4) and GF(8) codes, respectively. As we can see, the difference in performance for both codes beyond the sixth iteration is insignificant. Due to the relatively high BER range of interest, the asymptotic achievable diversity order of 8 and 12 for GF(4) and GF(8) codes are not evident in results obtained. However, a diversity loss of order $LN_R = 4$ is to be expected between GF(4) and GF(8) codes. This diversity loss can indeed be observed in the results obtained. From the figures, the achieved diversity order for GF(4) and GF(8) codes is six and ten, respectively. Due to the diminishing returns in the performance, as well as the high complexity involved in the iterative process, only six iterations will be performed for our subsequent simulations. However, bear in mind that improvement in the performance can still be obtained by increasing the number of iterations.

Fig. 4 shows the BER peformance of GF(4) codes with $L = 2$ and $N_R = 2$ at various frame length N. As the figure shows, the total achievable diversity order is slightly decreased with shorter frame lengths. This is because of the nature of the turbo concept, where randomness of the codeword does improve the performance. In other words, with a short frame length, the mutual information of the decoder feedback cannot reach a point required to convert the L-path channels to the equivalent LN_R flat channels by the JA-MMSE detector. In this case, the JA-MMSE detector has to use its degrees-of-freedom to cancel the residual interference, resulting in a decrease in the diversity order. On the other hand, as noted in [14], the diversity order

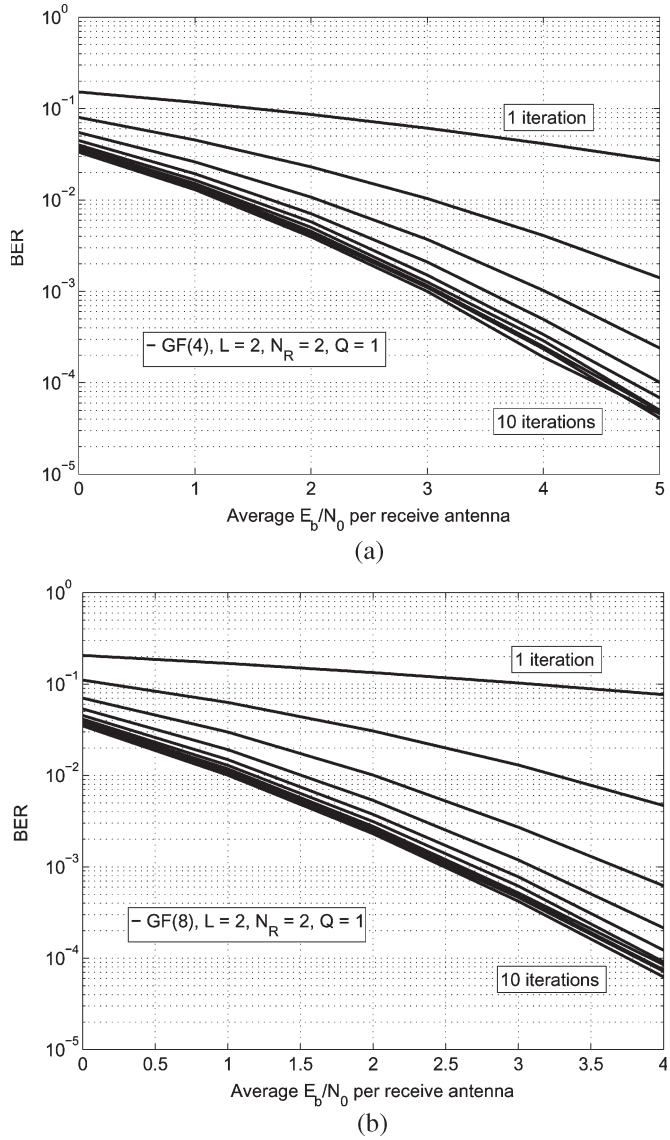

Fig. 3. BER performance versus the number of iterations for $L = 2$, $N_R = 2$, and $Q = 1$. (a) GF(4) ST-WNRA codes. (b) GF(8) ST-WNRA codes.

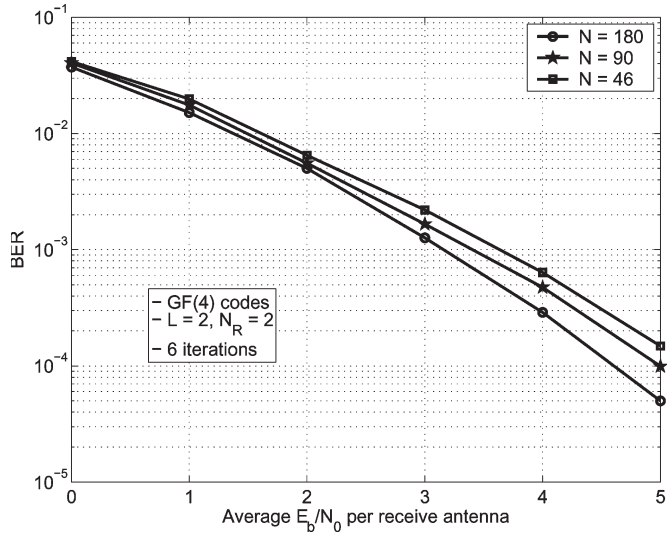

Fig. 4. Performance comparison of GF(4) ST-WNRA codes for different frame lengths with $L = 2$ and $N_R = 2$.

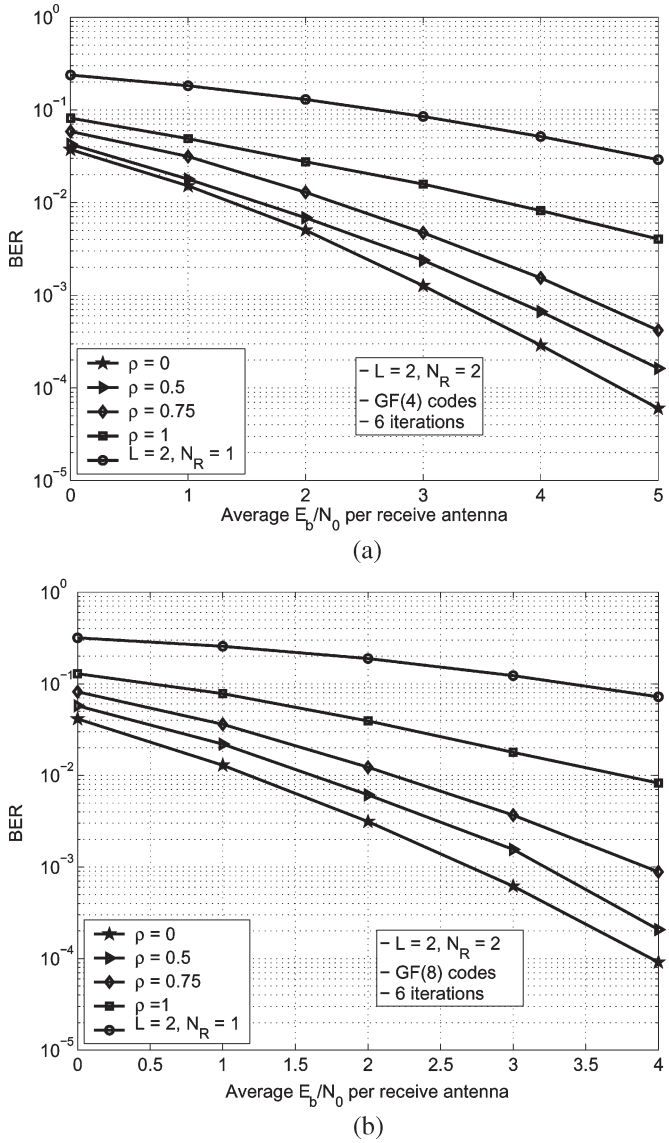

Fig. 5. BER performance on correlated flat fading channels with $N_R = 2$ and $Q = 1$. (a) GF(4) ST-WNRA codes. (b) GF(8) ST-WNRA codes.

of the ST-WNRA code is related to the size of the GF, and in order to satisfy the rank requirement of the code, the interleaver length has to be as large as the number of primitive elements of the GF, which is relatively small. The means that the maximum diversity order can be asymptotically achieved even with a short frame length.

Fig. 5(a) and (b) shows the performance of GF(4) and GF(8) codes, respectively, in correlated Rayleigh fading channel with $L = 2$ and $N_R = 2$. The correlation coefficient ρ between the two receive antennas, as given by (12), are chosen to be 0, 0.5, 0.75, and 1.0. The BER performances of these codes with $L = 2$ and $N_R = 1$ are also shown in the figures for comparison sake. As we can see when $\rho = 0.5$, there is only a slight degradation in the performance as compared to the uncorrelated case, i.e., $\rho = 0$. However, as the correlation between the receive antennas increases, the performance is degraded. In fact, when the receive antennas are fully correlated, i.e., $\rho = 1$, the benefit of having the receive antenna diversity no longer exists. In this

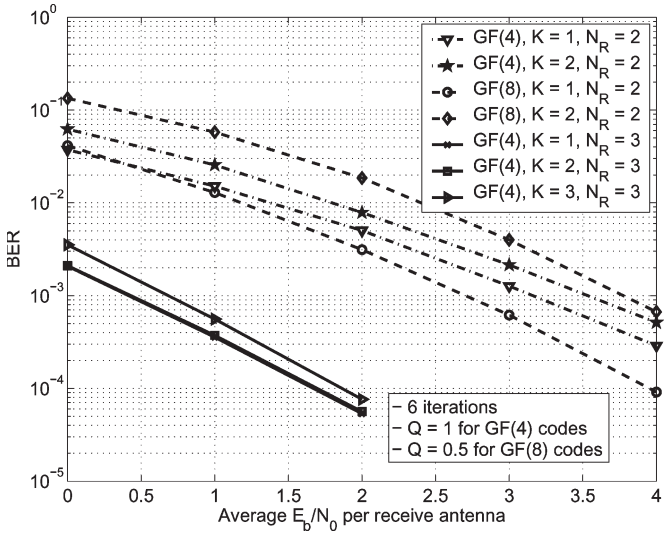

Fig. 6. Performance comparison of GF(4) and GF(8) ST-WNRA codes with various number of users and receive antennas, and $L = 2$.

case, the achievable diversity gain is only due to the ST-WNRA codes and the multipath components. As shown in Fig. 5(a) and (b), the slopes of GF(4) and GF(8) codes for $\rho = 1$ is similar as that for $L = 2$ and $N_R = 1$ but are shifted by 3 dB due to the additional antenna gain, thus achieving the same order of diversity.

B. Multiuser Performance

After having seen the performance of the system in a single-user scenario, let us now examine the performance under a multiple-user environment. We have assumed that all the users transmit with the same average power.

Fig. 6 shows the performance of the proposed system with multiple users for GF(4) and GF(8) ST-WNRA codes. For comparison, the single-user BER performance under the same system conditions is also shown. The Q-value is set to 0.5 for GF(8) codes, as we observed that this value gives a better performance. As shown in Fig. 6, with two users and two receive antennas, the BER performance degrades by about 0.5 and 1 dB for GF(4) and GF(8) codes, respectively, relative to the single-user bound. On the other hand, when there are three receive antennas, the BER performance with two users approaches the single-user bound. This is because the additional antennas are able to preserve the degrees of freedom of the JA-MMSE detector that can be used to cancel the other users' signals [15]. We can also observe that the BER degrades by about 0.25 dB with three users. More importantly, however, we observed that the slope of the curves with multiple users is the same as that of the corresponding single-user case [15]. This implies that the achievable diversity order is maintained, regardless of the number of users present, as long as $N_R \leq K$. We can also see that the slope of curves corresponding to GF(4) codes with three receive antennas is the same as that with GF(8) codes having two receive antennas. This conforms to our proposition that the achievable diversity order of our system is indeed given by $N_T \times L \times N_R$.

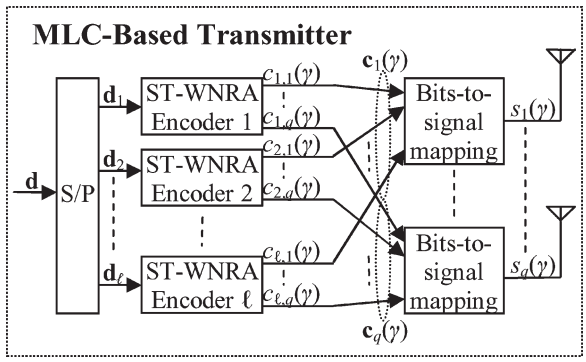

Fig. 7. Transmitter model of the multilevel-coded modulation based on GF(2^q) ST-WNRA codes.

V. Multilevel ST-WNRA-Coded Modulation

In Section II, the bandwidth efficiency of the proposed system is essentially limited, since BPSK was used as the underlying modulation method for the ST-WNRA codes in order to achieve the desired full transmit diversity. In this section, we will show that the ST-WNRA codes can also achieve full transmit diversity with higher modulation alphabet by incorporating the multilevel-coding (MLC) concept so that the bandwidth efficiency of our proposed system is not bounded by the ST-WNRA code's binary-mapping part. Furthermore, our MLC-based system is designed in such a way that it is similar to that highlighted in our previous sections so that the maximum diversity order can also be achieved. MLC [31]–[38] has long been recognized as an efficient scheme for transmitting information through bandwidth-constrained channels. The basic idea behind MLC is to partition a signal set into several levels and each level is separately encoded with an appropriate component code. However, to the best of our knowledge, achieving the maximum diversity order in the MLC regime has yet to appear in the literature.

A. System Model

The transmitter of a GF(2^q) ST-WNRA-coded MLC scheme with M-ary transmission is shown in Fig. 7. For simplicity sake and without loss of generality, only a single user will be considered here. At the transmitter, a frame consisting of N_BGF(2^q) information symbols $\mathbf{d} = [d(1), \ldots, d(N_B)]$, $d(\iota) \in \{0, 1\}$ is first serial-to-parallel converted into ℓ number of component information subsequences $\mathbf{d}_i = [d_i(1), \ldots, d_i(N_{B_i})]$, $i = 1, \ldots, \ell$, where $\ell = \log_2 M$ denotes the number of levels present in the system, and N_{B_i} is the length of each subsequence such that $\sum_{i=1}^{\ell} N_{B_i} = N_B$. The subsequence in each level is then fed into an individual ST-WNRA encoder, as shown in Fig. 7. Similar to (1), the ith level's ST-WNRA component codeword is expressed as

$$\mathbf{C}_i = \begin{bmatrix} c_{i,1}(1) & c_{i,1}(2) & \cdots & c_{i,1}(r_i N_{B_i}) \\ \vdots & \vdots & \ddots & \vdots \\ c_{i,q}(1) & c_{i,q}(2) & \cdots & c_{i,q}(r_i N_{B_i}) \end{bmatrix} \tag{28}$$

where $c_{i,j}(\gamma) \in \{-1, 1\}$, with r_i denoting the number of symbol repetitions at the ith level. By varying the values of

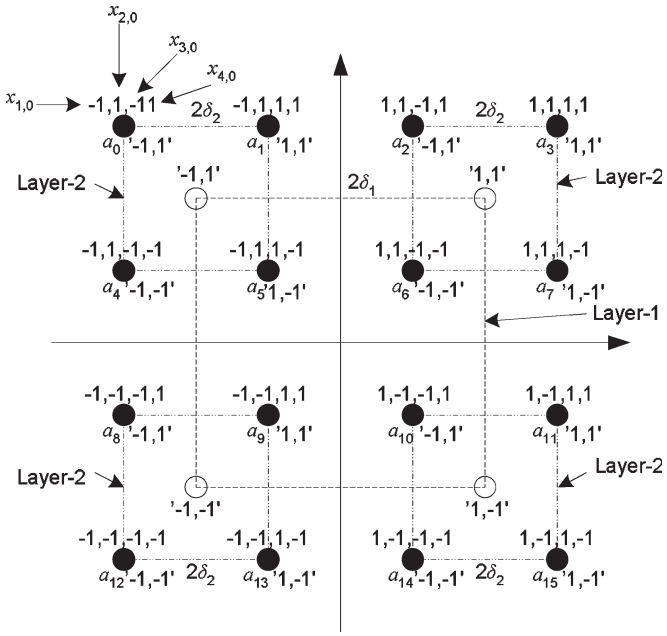

Fig. 8. Hierarchical block-partitioned 16-QAM constellation.

r_i for each level, subject to the constraint that $r_i N_{B_i}$ should be the same for all levels, equal-error-protection (EEP) coding scheme as well as unequal-error-protection (UEP) coding scheme among the multiple levels can be easily implemented. Since the rate of $\mathbf{C}_i$ is given by q/r_i, as highlighted in Section II, the overall bandwidth efficiency η of the scheme is equal to the sum of the individual component code rate, namely $\eta = \sum_{i=1}^{\ell} R_i = \sum_{i=1}^{\ell} (q/r_i)$.

The bits-to-symbol mapping function in Fig. 7, is based on the hierarchical BP of a $M = 16$-QAM constellation [37], [39], which is illustrated in Fig. 8. Each signal point in the constellation is taken from the signal set $\mathcal{A} = \{a_0, \ldots, a_{M-1}\}$. We can view this constellation as having four clusters, with one in each quadrant. Each cluster consists of four signal points and the center of each cluster is represented by a fictitious signal point, which is denoted by a white circle in Fig. 8. These four fictitious signal points form a 4-QAM constellation having a minimum squared Euclidean distance (MSED) δ_1. Similarly, the four signal points in each cluster also form a 4-QAM constellation having an MSED δ_2. All the signal points are assigned with a unique ℓ-bit address vector, denoted here as $(x_{1,k}, \ldots, x_{\ell,k})$, $k = 0, \ldots, M-1$, where $x_{i,k} \in \{-1, 1\}$. As shown in Fig. 8, the address vectors of these signal points are labeled with respect to their nearest fictitious signal point $(x_{1,k}, x_{2,k})$ as well as their position within their associated cluster $(x_{3,k}, x_{4,k})$.

According to Fig. 7, the codeword symbols $c_{i,j}(\gamma)$ corresponding to the jth row of $\mathbf{C}_i$ for all levels at time instant γ will form a binary label $\mathbf{c}_j(\gamma) = [c_{1,j}(\gamma), \ldots, c_{\ell,j}(\gamma)]$ at the input of the jth mapper. This binary label is then mapped to a signal point a_k such that $c_{i,j}(\gamma) = x_{i,k}$ for all i. More explicitly, the output symbols of the first- and second-level codewords $(c_{1,j}(\gamma), c_{2,j}(\gamma))$ will select one of the four clusters, whereas the output symbols of the third- and fourth-level codewords $(c_{3,j}(\gamma), c_{4,j}(\gamma))$ will select one of the four signal points in the chosen cluster. Subsequently, in our discourse herein, levels 1 and 2 will be referred to as Layer-1 and levels 3 and 4 as Layer-2. We shall denote the signal point addressed by $\mathbf{c}_j(\gamma)$ as $s_j(\gamma) \in \mathcal{A}$ at the output of the jth BP mapper at time γ.

Alternatively, the mapping function can be simply expressed as a multiplication between the binary label $\mathbf{c}_j(\gamma)$ and a complex weight vector $\mathbf{z} = [z_1, \ldots, z_\ell]$ as follows [37]:

$$s_j(\gamma) = \mathbf{z}\mathbf{c}_j^T(\gamma) \tag{29}$$

where the elements z_m are real if m is odd and $z_m = iz_{m-1}$ if m is even. The elements in $\mathbf{z}$ are also normalized such that $\mathbf{z}^H\mathbf{z} = 1$.

In general, for a GF(2^q) ST-WNRA-coded-multilevel scheme, there will be q number of BP mappers in our proposed system, resulting in q number of independent M-ary symbols at each time instant. These symbols $s_1(\gamma), \ldots, s_q(\gamma)$ will be transmitted synchronously from their respective antennas at that time instant, as depicted in Fig. 7. Hence, the number of transmit antennas N_T equals q.

Based on the spatially independent channel as highlighted in Section II-A, the space-time received-signal vector can be written as

$$\begin{aligned}\mathbf{y}(i) &= \mathbf{H}\mathbf{s}(i) + \mathbf{n}(i) \\ &= \underbrace{\mathbf{H}\mathbf{Z}}_{\bar{\mathbf{H}}}\mathbf{b}(i) + \mathbf{n}(i)\end{aligned} \tag{30}$$

where $\mathbf{H}$ is given in (7) with one user, $\mathbf{s}(i) = [s_1(i+L-1), \ldots, s_{N_T}(i+L-1), \ldots, s_{N_T}(i-L+1\,l)]^{\mathrm{T}}$, $\mathbf{b}(i) = [\tilde{\mathbf{c}}_1(i+L-1), \ldots, \tilde{\mathbf{c}}_{N_T}(i-L+1)]^{\mathrm{T}}$, $\mathbf{Z} = (\mathbf{I}_{(2L-1)N_T} \otimes \mathbf{z})$, and $\otimes$ denotes a Kronecker product. The product $\mathbf{HZ}$ can be interpreted as a hypothetical channel, which is the concatenation of the mapping function and the propagation channel, and it will be denoted as $\bar{\mathbf{H}}$. Hence, the received signal $\mathbf{y}(i)$ can be viewed as a vector of BPSK modulated symbols $\mathbf{b}(i)$ transmitted over a hypothetical channel $\bar{\mathbf{H}}$. This scenario is very similar to that shown in (6), where BPSK modulated signals from multiple independent users are transmitted over a common MIMO channel, and turbo equalization is performed on a user-by-user basis while treating the signals from the other undesired users as interference. Hence, by emulating the levels as virtual users, the turbo equalization technique with the JA-MMSE detector and ℓ number of ST-WNRA decoders, as highlighted in Section III, can also be used here, which should also achieve the maximum diversity order, as we shall see next.

B. Simulation Results

We investigate the performance of our proposed MLC-based system using both GF(4) and GF(8) ST-WNRA codes transmitted over a two-path Rayleigh fading channel. For GF(4) codes, $N_T = N_R = 2$, while for GF(8) codes, $N_T = N_R = 3$. The BER after eight iterations will be used as the performance measure. More explicitly, Layer-1 BER represents the rate of bit errors in the decoded subsequences $\hat{\mathbf{b}}_1$ and $\hat{\mathbf{b}}_2$, while Layer-2 BER represents the rate of bit errors in the decoded subsequences $\hat{\mathbf{b}}_3$ and $\hat{\mathbf{b}}_4$. The average BER will account for

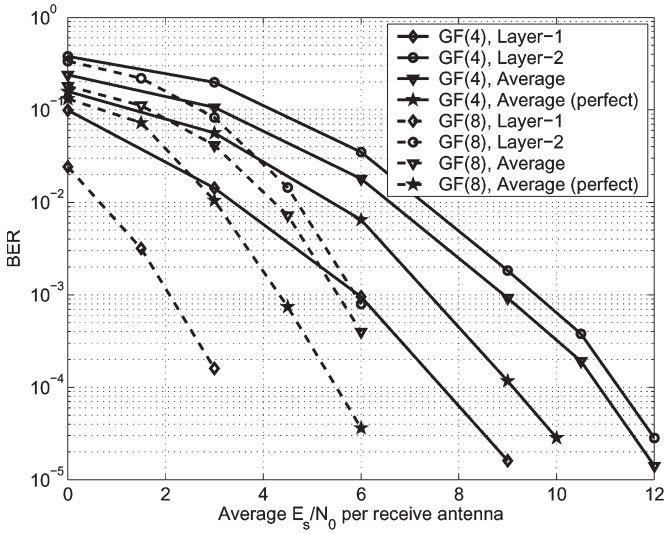

Fig. 9. Performance of GF(4) and GF(8) ST-WNRA codes with EEP.

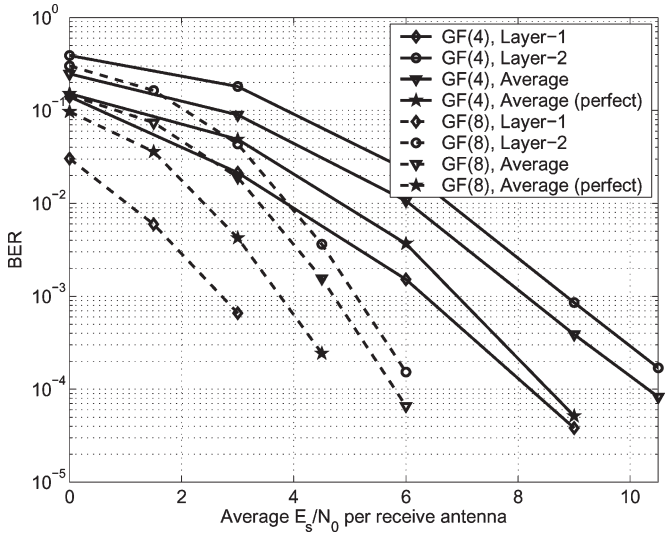

Fig. 10. Performance of GF(4) and GF(8) ST-WNRA codes with UEP.

the bit errors occurring in all the levels. The average BER with perfect feedback in the turbo equalization will also be shown for comparison. In other words, the soft decisions that are feedback from the decoders to the JA-MMSE detector correspond exactly to the transmitted symbols.

The BER performance under an EEP scenario is shown in Fig. 9, where $r_i = 3$ and $N_{B_i} = 180$ for all i. As we can see, the Layer-1 BER has about 4-dB gain over the Layer-2 BER for both GF(4) and GF(8) codes. This is due to the difference in the MSED between Layer-1 and Layer-2 constellations, as shown in Fig. 8. As a result, the average BER will largely be influenced by Layer-2 BER, which is degraded by about 1–2 dB as compared to that with perfect feedback. More importantly, close observation on the slope of the BER curves corresponding to the case with GF(4) codes reveals that a diversity order of eight is achieved for all layers at a BER below 10^{-4}. For the case of GF(8) codes, the expected diversity order is 12. The slope of the curves suggested that the performance should approach the expected diversity order at a lower BER. Also, the overall bandwidth efficiency with GF(4) and GF(8) codes is given by 8/3 and 4, respectively.

Let us now enhance the error-correcting capability of the Layer-2 codes by increasing r_i to four for $i = 3, 4$, while maintaining $r_i = 3$ for $i = 1, 2$. This corresponds to a UEP scenario. The overall bandwidth efficiency with GF(4) codes will be reduced to 7/3 and to 7/2 with GF(8) codes, for which the E_s/N_0 value is adjusted for the bandwidth expansion factor. The BER results are shown in Fig. 10. We can see that Layer-1 BER now has about less than 3-dB gain over the Layer-2 BER, which is an improvement of about 1 dB as compared to the previous case. Because of this, the average BER has also improved by about the same amount as compared to that shown in Fig. 9. On the other hand, the slope of the curves for the UEP case still remains the same as compared to the EEP case.

Fig. 11 showed how the BER and the bandwidth efficiency are affected by the repetition rate for GF(8) codes. The repetition for Layer-1 codes is fixed at three, while the repetition for Layer-2 codes varies from three to six. The results showed

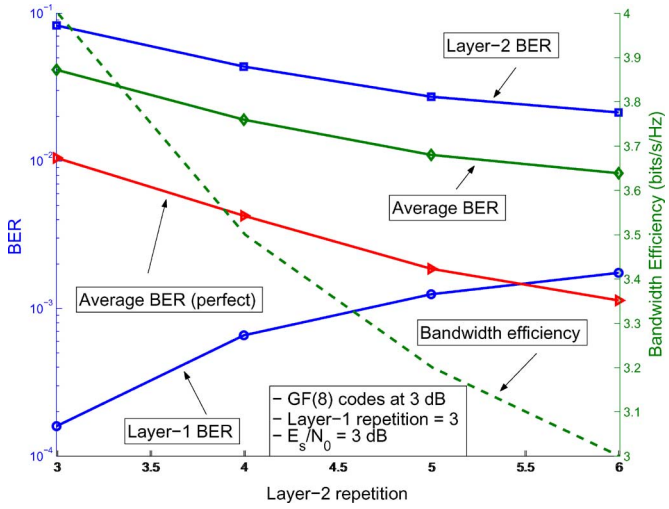

Fig. 11. BER performance and bandwidth efficiency of GF(8) ST-WNRA codes at various repetitions of Layer-2 codes.

that increasing the Layer-2 codes' repetition beyond six does not improve the BER significantly, even though the bandwidth efficiency decreases substantially. Similar BER deterioration is also observed with perfect feedback. Notice that the average BER performance difference between one with normal feedback and one with perfect feedback is quite large. This is due to the fact that the frame length of 180, as considered in our simulations for the multilevel transmission, is not long enough that is required to improve the decoder feedback mutual information in the JA-MMSE turbo equalization. Nevertheless, the considered frame length is still long enough for the system to achieve the maximum diversity order, as shown in Figs. 9 and 10. The same phenomenon was also observed for GF(4) codes, which was not shown here due to space constraints.

VI. Conclusion

We studied the performance of the ST-WNRA codes over a frequency-selective Rayleigh fading single-carrier MIMO channel in a multiuser environment. The JA-MMSE detector

Fig. 12. kth user's ST-WNRA encoder.

was designed so that the diversity that can be gleaned from the multiple antennas, as well as from the multipath components, can be fully exploited. It was demonstrated through computer simulations that the proposed system is capable of attaining the diversity gain obtained from the transmit and receive antennas, as well as the multipath components with relatively short frame lengths. Furthermore, the same achievable diversity order is maintained in a multiuser environment. We also proposed an MLC-based system that is also capable of offering a tradeoff between the BER performance and bandwidth efficiency while still achieving the maximum diversity order.

APPENDIX I
ST-WNRA ENCODER

The ST-WNRA encoder of each user consists of a repeater, a weighter, an outer interleaver, an accumulator, an inner interleaver, and a symbol-to-BPSK mapper, as shown in Fig. 12 for the kth user. The encoding and decoding of the ST-WNRA codes are performed on a frame-by-frame basis, where each frame consists of N number of uncoded information symbols. Each of these symbols corresponds to an element of GF(2^q), with q being a positive integer. Note that each symbol in turn corresponds to q number of information bits. Let $\mathbf{u}_k = [u_k(1), \ldots, u_k(N)]$ be a frame of N symbols corresponding to the kth user to be encoded, where $u_k(i) \in \{C_0, \ldots, C_{2^q-1}\}$. Each symbol in $\mathbf{u}_k$ is repeated r times, and the output is denoted by $\mathbf{x}_k = [x_k(1), \ldots, x_k(rN)]$, where $x_k(ir+j) = u_k(i+1)$ for $i = 0, \ldots, N-1$, $j = 1, \ldots, r$. The symbols in $\mathbf{x}_k$ are then modulo-GF(2^q) multiplied by their corresponding weights to produce $\mathbf{y}_k = [y_k(1), \ldots, y_k(rN)]$, where $y_k(i) = \beta(i) \otimes x_k(i)$, with $\beta(i) \in \{C_1, \ldots, C_{2^q-1}\}$ for $i = 1, \ldots, rN$ denoting the weight, and $\otimes$ is a modulo-GF(2^q) multiplication. The symbols in $\mathbf{y}_k$ are then interleaved in a random manner to produce the corresponding output $\mathbf{z}_k = [z_k(1), \ldots, z_k(rN)] = \prod_O(\mathbf{y}_k)$, where $\prod_O(\cdot)$ symbolizes the outer interleaving function. Finally, $\mathbf{z}_k$ is fed to the accumulator to produce the output $\tilde{\mathbf{c}}_k = [\tilde{c}_k(1), \ldots, \tilde{c}_k(rN)]$, where $\tilde{c}_k(i) = \tilde{c}_k(i-1) \oplus z_k(i), i = 1, \ldots, rN$ with $\tilde{c}_k(0) = 0$, and $\oplus$ denotes a modulo-GF(2^q) addition. Note that $\tilde{c}_k(i) \in \{C_0, \ldots, C_{2^q-1}\}$. The symbols in $\tilde{\mathbf{c}}_k$ are then interleaved by the inner interleaver, and the resulting output $\mathbf{c}_k = \prod_I(\tilde{\mathbf{c}}_k)$ is then mapped to its equivalent BPSK sequence $c_k(i) \triangleq [c_{k,1}(i), \ldots, c_{k,q}(i)]^{\mathrm{T}}$ for $i = 1, \ldots, rN$, where $\prod_I(\cdot)$ denotes the inner interleaving function, and $c_{k,j}(i) \in \{+1, -1\}$, $j = 1, \ldots, q$. Each BPSK-modulated symbol in $c_k(i)$ is then transmitted from a different antenna. Hence, $q = N_T$. We can expressed the kth user's ST-WNRA codeword as an $N_T \times rN$ matrix $\mathbf{C}_k$ as follows:

$$\mathbf{C}_k = \begin{bmatrix} c_{k,1}(1) & c_{k,1}(2) & \cdots & c_{k,1}(rN) \\ \vdots & \vdots & \ddots & \vdots \\ c_{k,N_T}(1) & c_{k,N_T}(2) & \cdots & c_{k,N_T}(rN) \end{bmatrix}. \quad (31)$$

APPENDIX II
SUM–PRODUCT ALGORITHM OF THE ST-WNRA DECODER

The structure of the kth user's ST-WNRA decoder is shown in Fig. 13(a).

Messages From the Check Nodes to the Deinterleaver: The input to the kth user ST-WNRA decoder are the *a priori* LLR vectors of the coded GF(2^q) symbols corresponding to that user, which were delivered from the JA-MMSE detector, as given in (25). The output messages from the check node decoder $\tilde{L}_k^{\langle j \rangle}(i)$, as shown in Fig. 13(b), are computed according to

$$\tilde{L}_k^{\langle j \rangle}(i) = \left[\lambda_{k,i}^{\langle j \rangle}(i-1) + \overrightarrow{L}_k^{\langle j \rangle}(i-1)\right] \odot \left[\lambda_k^{\langle j \rangle}(i) + \overleftarrow{L}_k^{\langle j \rangle}(i)\right], \qquad i = 1, \ldots, rN \quad (32)$$

where $\odot$ refers to a check operation, and the nth element in $\tilde{L}_k^{\langle j \rangle}(i)$ is calculated according to [14]

$$[\alpha \odot \beta]_n = \log \frac{\sum_{\gamma \in \{C_0, \ldots, C_{2^q-1}\}} \exp\left(\alpha(\gamma) + \beta(\gamma \oplus n)\right)}{\sum_{\gamma \in \{C_0, \ldots, C_{2^q-1}\}} \exp\left(\alpha(\gamma) + \beta(\gamma)\right)} \qquad n = 0, \ldots, 2^q - 1. \quad (33)$$

where $[\alpha \odot \beta]_n$ refers to the nth element of the vector denoted by $(\alpha \odot \beta)$, with $\alpha(\gamma)$ being the γth element in α. When $i = 1$, $\lambda_{k,i}^{\langle j \rangle}(0)$ and $\overrightarrow{L}_k^{\langle j \rangle}(0)$ in (32) are designated as zero vectors. The output messages $\tilde{L}_k^{\langle j \rangle}(i)$, $i = 1, \ldots, rN$ are then deinterleaved accordingly and fed to the deweighter, as denoted by $\bar{\tilde{L}}_k^{\langle j \rangle}(i)$ in Fig. 13(a).

Messages From the Check Nodes to the Parity Nodes: The messages $\overrightarrow{L}_k^{\langle j \rangle}(i)$ and $\overleftarrow{L}_k^{\langle j \rangle}(i)$, which are required for the derivation of (32), are calculated according to

$$\overrightarrow{L}_k^{\langle j \rangle}(i) = \tilde{F}_k^{\langle j-1 \rangle}(i) \odot \left[\lambda_k^{\langle j \rangle}(i-1) + \overrightarrow{L}_k^{\langle j \rangle}(i-1)\right] \qquad i = 2, \ldots, rN \quad (34)$$

$$\overleftarrow{L}_k^{\langle j \rangle}(i) = \tilde{F}_k^{\langle j-1 \rangle}(i+1) \odot \left[\lambda_k^{\langle j \rangle}(i+1) + \overleftarrow{L}_k^{\langle (j) \rangle}(i+1)\right] \qquad i = 1, \ldots, (rN-1) \quad (35)$$

where $\tilde{F}_k^{\langle j-1 \rangle}(i)$ are the messages delivered by the information nodes, after the outer interleaver, during the previous iteration. At the first iteration, $\tilde{F}_k^{\langle 0 \rangle}(i)$ is a zero vector for $i = 1, \ldots, rN$. Also, $\overrightarrow{L}_k^{\langle j \rangle}(1) = \tilde{F}_k^{\langle j \rangle}(1)$, and $\overleftarrow{L}_k^{\langle j \rangle}(rN)$ is a zero vector in (34) and (35), respectively.

Deweighter: The deweighter, shown in Fig. 13(a), simply performs a cyclic shift of the elements in the input message

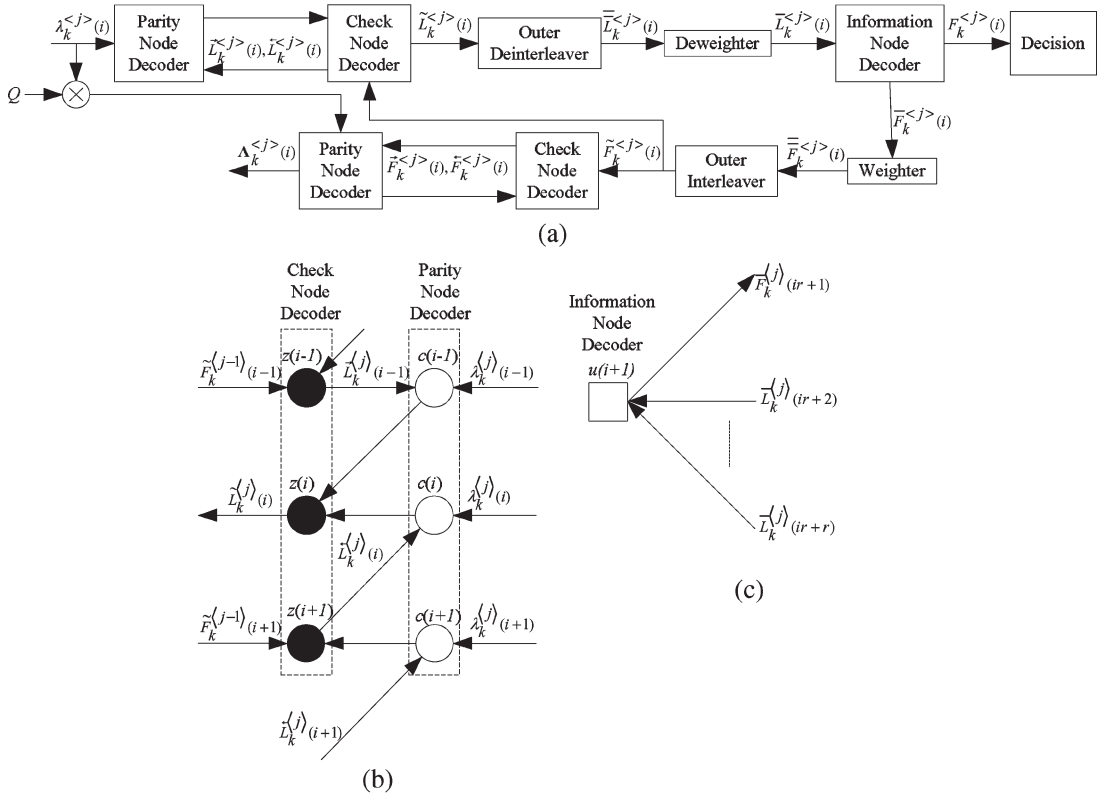

Fig. 13. (a) kth user's ST-WNRA decoder. (b) Factor graph representation of the accumulator. (c) Factor-graph representation of the repeater.

$\bar{\bar{L}}_k^{\langle j\rangle}(i)$ according to the weighting value $\beta(i)$, except for the element $\bar{\bar{L}}_k^{\langle j\rangle}(i,0)$, in order to produce the message $\bar{L}_k^{\langle j\rangle}(i)$. For example, if $\beta(i)=1$, then

$$\bar{L}_k^{\langle j\rangle}(i)=\Big[\bar{\bar{L}}_k^{\langle j\rangle}(i,0),\bar{\bar{L}}_k^{\langle j\rangle}(i,2^q-1)\;\bar{\bar{L}}_k^{\langle j\rangle}(i,1),\ldots,\bar{\bar{L}}_k^{\langle j\rangle}(i,2^q-2)\Big].$$

The deweighted messages $\bar{L}_k^{\langle j\rangle}(i)$, $i=1,\ldots,rN$ are then fed to the information nodes.

Messages and Decisions From the Information Nodes: The information node corresponding to the $(i+1)$th information symbol is shown in Fig. 13(c). If the jth iteration is not the last iteration, then the output messages from the information nodes $\bar{F}_k^{\langle j\rangle}(i)$ are calculated according to

$$\bar{F}_k^{\langle j\rangle}(ir+x)=\sum_{y=1,y\neq x}^{r}\bar{L}_k^{\langle j\rangle}(ir+y)\qquad i=0,\ldots,(N-1)\ \text{ and }\ x=1,\ldots,r. \quad (36)$$

On the other hand, if the jth iteration is the last iteration, then a decision on the $(i+1)$th uncoded information symbol is made based on the highest value LLR element in $F_k^{\langle j\rangle}(i+1)$, where

$$F_k^{\langle j\rangle}(i+1)=\sum_{y=1}^{r}\bar{L}_k^{\langle j\rangle}(ir+y)\qquad i=0,\ldots,(N-1). \quad (37)$$

Messages to the JA-MMSE Detector: Following the computation of the message $\bar{F}_k^{\langle j\rangle}(i)$ in (36), the elements in the message are again cyclic shifted, but in the reverse direction, by the weighter and interleaved to obtain $\tilde{F}_k^{\langle j\rangle}(i)$. The extrinsic information from the kth user's ST-WNRA decoder to the JA-MMSE detector $\Lambda_k^{\langle j\rangle}(i)$ are then derived according to

$$\Lambda_k^{\langle j\rangle}(i)=\Big[Q\times\lambda_k^{\langle j\rangle}(i)\Big]+\overleftarrow{F}_k^{\langle j\rangle}(i)+\overrightarrow{F}_k^{\langle j\rangle}(i)\qquad i=1,\ldots,rN \quad (38)$$

where

$$\overrightarrow{F}_k^{\langle j\rangle}(i)=\tilde{F}_k^{\langle j\rangle}(i)\odot\Big[\lambda_k^{\langle j\rangle}(i-1)+\overrightarrow{F}_k^{\langle j\rangle}(i-1)\Big]\qquad i=2,\ldots,rN \quad (39)$$

$$\overleftarrow{F}_k^{\langle j\rangle}(i)=\tilde{F}_k^{\langle j\rangle}(i+1)\odot\Big[\lambda_k^{\langle j\rangle}(i+1)+\overleftarrow{F}_k^{(j)}(i+1)\Big]\qquad i=1,\ldots,(rN-1). \quad (40)$$

Following [9], a scaling factor Q is also introduced in (38) to enhance the iterative processing performance. However, notice that the scaled input extrinsic information $Q\times\lambda_k^{\langle j\rangle}(i)$ is added to the output extrinsic information $\Lambda_k^{\langle j\rangle}(i)$, instead of subtracting from it, as found in [9]. This is due to the fact that the original input extrinsic information was omitted in the feedback path leading to the derivation of the corresponding output extrinsic information, as we have deduced from (36).

REFERENCES

[1] I. E. Telatar, "Capacity of multi-antenna Gaussian channels," *Eur. Trans. Telecommun.*, vol. 10, no. 6, pp. 585–595, Nov. 1999.

[2] G. J. Foschini and M. J. Gans, "On limits of wireless communications in a fading environment when using multiple antennas," *Wireless Pers. Commun.*, vol. 6, no. 3, pp. 311–335, Mar. 1998.

[3] V. Tarokh, N. Seshadri, and A. R. Calderbank, "Space-time codes for high data rate wireless communication: Performance criterion and code construction," *IEEE Trans. Inf. Theory*, vol. 44, no. 2, pp. 744–765, Mar. 1998.

[4] S. M. Alamouti, "A simple transmitter diversity scheme for wireless communications," *IEEE J. Sel. Areas Commun.*, vol. 16, no. 8, pp. 1451–1458, Oct. 1998.

[5] Y. Gong and K. B. Letaief, "Performance evaluation and analysis of space-time coding in unequalized multipath fading links," *IEEE Trans. Commun.*, vol. 48, no. 11, pp. 1778–1782, Nov. 2000.

[6] S. Zhou and G. B. Giannakis, "Single-carrier space-time block-coded transmissions over frequency-selective fading channels," *IEEE Trans. Inf. Theory*, vol. 49, no. 1, pp. 164–179, Jan. 2003.

[7] M. Qin and R. S. Blum, "Properties of space-time codes for frequency-selective channels," *IEEE Trans. Signal Process.*, vol. 52, no. 3, pp. 694–702, Mar. 2004.

[8] H. Bölcskei and A. J. Paulraj, "Space-frequency coded broadband OFDM systems," in *Proc. Wireless Commun. and Netw. Conf.*, Chicago, IL, Sep. 2000, vol. 1, pp. 1–6.

[9] B. Lu and X. Wang, "Space-time code design in OFDM systems," in *Proc. Global Telecommun. Conf.*, San Francisco, CA, 2000, vol. 2, pp. 1000–1004.

[10] Z. Liu, Y. Xin, and G. B. Giannakis, "Space-time–frequency coded OFDM over frequency-selective fading channels," *IEEE Trans. Signal Process.*, vol. 50, no. 10, pp. 2465–2476, Oct. 2002.

[11] Z. Wang, X. Ma, and G. B. Giannakis, "OFDM or single-carrier block transmissions?" *IEEE Trans. Commun.*, vol. 52, no. 3, pp. 380–394, Mar. 2004.

[12] E. Lindskog and A. J. Paulraj, "A transmit diversity scheme for channels with intersymbol interference," in *Proc. Int. Conf. Commun.*, vol. 1. New Orleans, LA, Jun. 2000, pp. 307–311.

[13] R. Schober, W. H. Gerstacker, and L. H.-J. Lampe, "Performance analysis and design of STBCs for frequency-selective fading channels," *IEEE Trans. Wireless Commun.*, vol. 3, no. 3, pp. 734–744, May 2004.

[14] J.-E. Oh and K. Yang, "Space-time codes with full antenna diversity using weighted nonbinary repeat-accumulate codes," *IEEE Trans. Commun.*, vol. 51, no. 11, pp. 1773–1778, Nov. 2003.

[15] N. Veselinovic and T. Matsumoto, "Space-time coded turbo equalization and multiuser detection—Asymptotic performance analysis in the presence of unknown interference," in *Proc. Asilomar Conf. Signals, Syst., Comput.*, Nov. 7–10, 2004, vol. 1, pp. 1183–1187.

[16] W. Choi and J. M. Cioffi, "Space-time block codes over frequency-selective Rayleigh fading channels," in *Proc. IEEE Veh. Technol. Conf.*, Amsterdam, The Netherlands, Sep. 1999, vol. 5, pp. 2541–2545.

[17] G. Bauch and N. Al-Dhahir, "Reduced-complexity space-time turbo-equalization for frequency-selective MIMO channels," *IEEE Trans. Wireless Commun.*, vol. 1, no. 4, pp. 819–828, Oct. 2002.

[18] X. Wautelet, A. Dejonghe, and L. Vandendorpe, "MMSE-based fractional turbo receiver for space-time BICM over frequency-selective MIMO fading channels," *IEEE Trans. Signal Process.*, vol. 52, no. 6, pp. 1804–1809, Jun. 2004.

[19] N. Al-Dhahir, "Overview and comparison of equalization schemes for space-time-coded signals with application to EDGE," *IEEE Trans. Signal Process.*, vol. 50, no. 10, pp. 2477–2488, Oct. 2002.

[20] H. Bölcskei and A. J. Paulraj, "Performance of space-time codes in the presence of spatial fading correlations," in *Proc. Asilomar Conf.*, Sep. 2000, pp. 687–693.

[21] J. Wang, M. K. Simon, M. P. Fitz, and K. Yao, "On the performance of space-time codes over spatially correlated Rayleigh fading channels," *IEEE Trans. Commun.*, vol. 52, no. 6, pp. 877–881, Jun. 2004.

[22] J. P. Kermoal, L. Schumacher, K. I. Pedersen, P. E. Mogensen, and F. Frederiksen, "A stochastic MIMO radio channel model with experimental validation," *IEEE J. Sel. Areas Commun.*, vol. 20, no. 6, pp. 1211–1226, Aug. 2002.

[23] X. Wang and H. V. Poor, "Iterative (turbo) soft interference cancellation and decoding for coded CDMA," *IEEE Trans. Commun.*, vol. 47, no. 7, pp. 1046–1061, Jul. 1999.

[24] T. Abe and T. Matsumoto, "Space-time turbo equalization in frequency-selective MIMO channels," *IEEE Trans. Veh. Technol.*, vol. 52, no. 3, pp. 469–475, May 2003.

[25] R. G. Gallager, *Low-Density Parity-Check Codes*. Cambridge, MA: MIT Press, 1963.

[26] D. Tujkovic, M. Juntti, and M. Latva-aho, "Space-frequency-time turbo coded modulation," *IEEE Commun. Lett.*, vol. 5, no. 12, pp. 480–482, Dec. 2001.

[27] H.-N. Lee and V. Gulati, "Iterative equalization/decoding of LDPC code transmitted over MIMO fading ISI channels," in *Proc. IEEE Int. Symp. Pers., Indoor, and Mobile Radio Commun.*, Lisbon, Portugal, Sep. 2002, vol. 3, pp. 1330–1336.

[28] J. Karjalainen, N. Veselinovic, K. Kansanen, and T. Matsumoto, "Iterative frequency domain joint-over-antenna receiver for multiuser MIMO," in *Proc. 4th Int. Symp. Turbo Codes*, Munich, Germany, Apr. 3–7, 2006, 6 p.

[29] J. Karjalainen, C. Schneider, K. Yen, M. Grossmann, T. Matsumoto, and R. Thoma, "Evaluation of joint over antenna detection with ST-WNRA coded MU MIMO transmission in realistic channels," in *Proc. ITG Workshop Smart Antennas*, Ulm, Germany, Mar. 13–14, 2006, 6 p.

[30] J. Li, K. R. Narayanan, and C. N. Georghiades, "Product accumulate codes: A class of codes with near-capacity performance and low decoding complexity," *IEEE Trans. Inf. Theory*, vol. 50, no. 1, pp. 31–46, Jan. 2004.

[31] H. Imai and S. Hirakawa, "A new multilevel coding method using error correcting codes," *IEEE Trans. Inf. Theory*, vol. IT-23, no. 3, pp. 371–377, May 1977.

[32] U. Wachsmann, R. F. H. Fischer, and J. B. Huber, "Multilevel codes: Theoretical concepts and practical design rules," *IEEE Trans. Inf. Theory*, vol. 45, no. 5, pp. 1361–1391, Jul. 1999.

[33] R. H. Morelos-Zaragoza, M. P. C. Fossorier, S. Lin, and H. Imai, "Multilevel coded modulation for unequal error protection and multistage decoding—Part I: Symmetric constellations," *IEEE Trans. Commun.*, vol. 48, no. 2, pp. 204–213, Feb. 2000.

[34] K. O. Holdsworth, D. P. Taylor, and R. T. Pullman, "On combined equalization and decoding of multilevel coded modulation," *IEEE Trans. Commun.*, vol. 49, no. 6, pp. 943–947, Jun. 2001.

[35] J. Hou, P. H. Siegel, L. B. Milstein, and H. D. Pfister, "Capacity-approaching bandwidth-efficient coded modulation schemes based on low-density parity-check codes," *IEEE Trans. Inf. Theory*, vol. 49, no. 9, pp. 2141–2155, Sep. 2003.

[36] P. Limpaphayom and K. A. Winick, "Power- and bandwidth-efficient communications using LDPC codes," *IEEE Trans. Commun.*, vol. 52, no. 3, pp. 350–354, Mar. 2004.

[37] K. Kansanen, C. Schneider, T. Matsumoto, and R. Thomä, "Multilevel coded QAM with MIMO turbo-equalization in broadband single-carrier signaling," *IEEE Trans. Veh. Technol.*, vol. 54, no. 3, pp. 954–966, May 2005.

[38] L. H.-J. Lampe, R. Schober, and R. F. H. Fischer, "Multilevel coding for multiple-antenna transmission," *IEEE Trans. Wireless Commun.*, vol. 3, no. 1, pp. 203–208, Jan. 2004.

[39] P. K. Vitthaladevuni and M.-S. Alouini, "A recursive algorithm for the exact BER computation of generalized hierarchical QAM constellations," *IEEE Trans. Inf. Theory*, vol. 49, no. 1, pp. 297–307, Jan. 2003.

Kai Yen received the B.Eng. degree (with first-class honors) in electronics engineering from the Nanyang Technological University, Singapore, in 1996 and the Ph.D. degree in mobile communications from the University of Southampton, Southampton, U.K., in 2001.

Since 2001, he has been working with the Institute for Infocomm Research, Singapore, as a Senior Research Fellow. In 2004–2006, he was a Visiting Researcher at the Centre for Wireless Communications, Oulu, Finland. His current research interests include multiple-input–multiple-output systems, channel coding, and turbo-equalization schemes.

Nenad Veselinovic (S'99–M'05) was born in Serbia in 1975. He received the M.S. degree from the University of Belgrade, Belgrade, Serbia, in 1999 and the Dr.Sc. (Tech.) degree from the University of Oulu, Oulu, Finland, in 2004.

During 2000–2005, he was with the Centre for Wireless Communications, University of Oulu, where he has worked on various projects as a Research Scientist and Project Manager. Since January 2006, he has been with Elektrobit Ltd., Kauniainen, Finland. He has authored and coauthored more than 20 papers in international conferences and journals. His research interests are in the general areas of statistical signal processing and transceiver design for wireless communications.

Kimmo Kansanen received the M.Sc. and Dr.Sc. degrees from the University of Oulu, Oulu, Finland, in 1998 and 2005, respectively.

He is currently working with the Centre for Wireless Communications, University of Oulu, as a Project Manager and Research Engineer. His research interests include joint iterative detection and decoding, co-operative communications in wireless networks, and communication theory.

Tadashi Matsumoto (M'84–SM'95) received the B.S., M.S., and Ph.D. degrees from Keio University, Yokohama, Japan, in 1978, 1980, and 1991, respectively, all in electrical engineering.

He joined Nippon Telegraph and Telephone Corporation (NTT) in April 1980. From April 1980 to May 1987, he researched signal-transmission technologies, such as modulation/demodulation schemes, as well as radio link design for mobile communications systems. He participated in the R&D project of NTT's high-capacity mobile communications system. From May 1987 to February 1991, he researched error-control strategies for digital mobile radio channels. He was involved in the development of a Japanese Time-Division Multiple-Access Digital Cellular Mobile Communications System called Personal Digital Cellular (PDC). In July 1992, he transferred to NTT DoCoMo, Inc. From February 1991 to April 1994, he worked on Code-Division Multiple-Access Mobile Communication Systems. From 1992 to 1994, he served as a part-time Lecturer at Keio University. In April 1994, he transferred to NTT America, where he served as a Senior Technical Advisor of a joint project between NTT and NEXTEL Communications. In March 1996, he returned to NTT DoCoMo, where he was the Head of the Radio Signal Processing Laboratory until August of 2001, when he worked on adaptive signal processing, multiple-input–multiple-output turbo signal detection, interference cancellation, and space-time coding techniques for broadband mobile communications. In May 2002, he moved to Oulu University, Oulu, Finland, where he is currently a Professor with the Center for the Wireless Communications. He was serving as a Visiting Professor at Ilmenau University of Technology, Ilmenau, Germany, funded by the German MERCATOR Visiting Professorship Program, until mid-January 2007.

Dr. Matsumoto, with the IEEE Vehicular Technology Society's recognition of his hard work for the organization of the 2000 Spring IEEE Vehicular Technology Conference (VTC2000-Spring) in Tokyo, is the recipient of an Outstanding Service Award. He served as a member of the Board-of-Governors of the IEEE Vehicular Technology Society from January 2002 to December 2004 and is now serving from January 2005 to December 2007.